



**HAL**  
open science

## Mechanisms underlying *Clostridium pasteurianum*'s metabolic shift when grown with *Geobacter sulfurreducens*

Roland Berthomieu, María Fernanda Pérez-Bernal, Gaëlle Santa-Catalina, Elie Desmond-Le Quéméner, Nicolas Bernet, Eric Trably

► **To cite this version:**

Roland Berthomieu, María Fernanda Pérez-Bernal, Gaëlle Santa-Catalina, Elie Desmond-Le Quéméner, Nicolas Bernet, et al.. Mechanisms underlying *Clostridium pasteurianum*'s metabolic shift when grown with *Geobacter sulfurreducens*. *Applied Microbiology and Biotechnology*, 2022, 106 (2), pp.865-876. 10.1007/s00253-021-11736-7 . hal-03516733

**HAL Id: hal-03516733**

**<https://hal.inrae.fr/hal-03516733>**

Submitted on 23 Feb 2022

**HAL** is a multi-disciplinary open access archive for the deposit and dissemination of scientific research documents, whether they are published or not. The documents may come from teaching and research institutions in France or abroad, or from public or private research centers.

L'archive ouverte pluridisciplinaire **HAL**, est destinée au dépôt et à la diffusion de documents scientifiques de niveau recherche, publiés ou non, émanant des établissements d'enseignement et de recherche français ou étrangers, des laboratoires publics ou privés.

# **Mechanisms underlying *Clostridium pasteurianum*'s metabolic shift when grown with *Geobacter sulfurreducens***

Roland Berthomieu<sup>1</sup>, María Fernanda Pérez-Bernal<sup>1</sup>, Gaëlle Santa-Catalina<sup>1</sup>, Elie Desmond-Le Quéméner<sup>1</sup>, Nicolas Bernet<sup>1</sup>, Eric Trably<sup>1,\*</sup>

<sup>1</sup>INRAE, Univ Montpellier, LBE, Narbonne, France.

\*eric.trably@inrae.fr

Roland Berthomieu's ORCID: 0000-0002-4413-0347

María Fernanda Pérez-Bernal's ORCID: 0000-0002-0316-7565

Elie Desmond-Le Quéméner's ORCID: 0000-0003-1675-2744

Nicolas Bernet's ORCID: 0000-0003-2710-3547

Eric Trably's ORCID: 0000-0002-7041-2962

## **Acknowledgments**

We are grateful to the Genotoul bioinformatics platform Toulouse Occitanie (Bioinfo Genotoul, doi: 10.15454/1.5572369328961167E12) for providing help, computing and storage resources.

This work was partly funded by Institut National de Recherche pour l'Agriculture, l'Alimentation et l'Environnement INRAE division Microbiologie Chaîne Alimentaire MICA.

Schemes were done using Smart Servier Medical Art (<https://smart.servier.com/>).

## ABSTRACT

Recently, a study showed that a glycerol fermentation by *Clostridium pasteurianum* could be metabolically redirected when the electroactive bacterium *Geobacter sulfurreducens* was added in the culture. It was assumed that this metabolic shift of the fermentative species resulted from an interspecies electron transfer. The aim of this study was to find out the mechanisms used for this interaction and how they affect the metabolism of *C. pasteurianum*. To get insights into the mechanisms involved, several coculture set-ups and RNA sequencing with differential expression analysis were performed. As a result, a putative interaction model was proposed: *G. sulfurreducens* produces cobamides molecules that possibly modify *C. pasteurianum* metabolic pathway at the key enzyme glycerol dehydratase, and affect its vanadium nitrogenase expression. In addition, the results suggested that *G. sulfurreducens*'s electrons could enter *C. pasteurianum* through its transmembrane flavin-bound polyferredoxin and cellular cytochrome b5 – rubredoxin interplay, putatively reinforcing the metabolic shift. Unravelling the mechanisms behind the interaction between fermentative and electroactive bacteria helps to better understand the role of bacterial interactions in fermentation set-ups.

**Keywords:** Cobalamin, RNAseq, *Clostridium pasteurianum*, *Geobacter sulfurreducens*, metabolic shift, interspecies electron transfer

### Keypoints:

- *C. pasteurianum* – *G. sulfurreducens* interaction inducing a metabolic shift is mediated
- *C. pasteurianum*'s metabolic shift in coculture might be induced by cobamides
- Electrons possibly enter *C. pasteurianum* through a multflavin polyferredoxin

## Introduction

Climate change is a major challenge to be urgently tackled. To limit global warming to 1.5 °C in 2100 compared to 1990, it was proposed to reach net-zero CO<sub>2</sub> emissions by 2050 (Rogelj et al. 2018). In this perspective, fossil fuels have to be partly replaced by liquid biofuels that are supposed to be multiplied by a factor of 4 by 2050 in the framework of the ‘Net-zero emission roadmap’ (IEA 2021). The synthesis of biodiesel, that represents the most important part of liquid biofuels, produces glycerol as a by-product. As a consequence, the production of glycerol (5 million tons in 2011 of which only 40 % was used according to Monteiro et al. 2018) is predicted to deeply increase in a near future. As a way of valorisation, glycerol can be biologically transformed by fermentation into several valuable compounds such as 1,3-propanediol, propionate or butanol that are useful energy or platform molecules (Monteiro et al. 2018).

Fermentation with mixed cultures can be used as an inexpensive way for waste valorisation, but bioprocess control is more difficult when compared to pure cultures. Strategies such as bioaugmentation (Okonkwo et al. 2020) or electrofermentation (Moscoviz et al. 2016) were proposed to control such fermentations. For example, addition of electrons with a poised electrode in a fermenter allowed for redirection of metabolic pathways towards ethanol in a mixed culture glycerol fermentation (+130 %; Moscoviz et al. 2018), and addition of *Clostridium acetobutylicum* led to higher yield in 1,3-propanediol (up to a 60 % increase) and induced ethanol production in a similar set-up (Dams et al. 2016). Mixed culture fermentations rely on a great number of microorganisms with considerable types of interactions that rule the process and the formation of end products. Understanding bacterial interactions is thus critical to trigger bioprocesses towards the production of specific compounds.

In previous studies, the glycerol-fermenting strain *Clostridium pasteurianum* was proven to divert its metabolic pathway from butanol to 1,3-propanediol in presence of a cathode (Choi et al. 2014) or with the bacterial partner *Geobacter sulfurreducens* (Moscoviz et al. 2017a). In the latter experience, *C. pasteurianum* was cultivated along with the model electroactive bacterium *G. sulfurreducens*, the former could ferment glycerol, but the latter lacked an electron acceptor to grow. *G. sulfurreducens* grew

though, suggesting that its electrons were transferred to *C. pasteurianum*. As a result of this forced interaction, the metabolic profile of the fermentative species shifted towards the production of propanediol at the expense of butanol, reaching a yield of  $0.2 \text{ g}_{\text{propanediol}} \cdot \text{g}_{\text{glycerol}}^{-1}$  (+37 %). However, the interaction mechanisms leading to such increase in 1,3-propanediol concentrations remain unknown. Neither a cellular molecular switch, nor any electron transfer system was suspected for *C. pasteurianum*, as the previously observed proteins involved in electron transfer such as c-type cytochromes (Faustino et al. 2021; Lovley 2017), flavin-based protein cluster (Light et al. 2018) or aerobic cytochrome bd (Pankratova et al. 2018; Paquete 2020) are not present in this species. Understanding the interaction mechanism between this fermentative species and electroactive species is interesting to better control mixed culture glycerol fermentation.

The present study aimed at characterizing the interaction between *C. pasteurianum* and *G. sulfurreducens* leading to a metabolic shift of the fermentative species. The preculture conditions favourable to this interaction were first investigated and RNA sequencing with differential expression analysis was then performed to unravel *C. pasteurianum*'s inward electron transfer system and the consequences on its metabolism.

## Materials and methods

### *Media*

Chemicals were purchased from Sigma Aldrich (Saint-Louis, USA) and were used for the following media.

Trace metal solution (for 1L): nitrilotriacetic acid, 1.5 g;  $\text{MgSO}_4 \cdot 7\text{H}_2\text{O}$ , 3 g;  $\text{MnSO}_4 \cdot \text{H}_2\text{O}$ , 0.5 g; NaCl, 1 g;  $\text{FeSO}_4 \cdot 7\text{H}_2\text{O}$ , 0.2 g;  $\text{CoSO}_4 \cdot 7\text{H}_2\text{O}$ , 0.18 g;  $\text{CaCl}_2 \cdot 2\text{H}_2\text{O}$ , 0.1 g;  $\text{ZnSO}_4 \cdot 7\text{H}_2\text{O}$ , 0.18 g;  $\text{CuSO}_4 \cdot 5\text{H}_2\text{O}$ , 0.01 g;  $\text{KAl}(\text{SO}_4)_2 \cdot 12\text{H}_2\text{O}$ , 0.02 g;  $\text{H}_3\text{BO}_3$ , 0.01 g;  $\text{Na}_2\text{MoO}_4 \cdot 2\text{H}_2\text{O}$ , 0.01 g;  $\text{NiCl}_2 \cdot 6\text{H}_2\text{O}$ , 0.03 g;  $\text{Na}_2\text{SeO}_3 \cdot 5\text{H}_2\text{O}$ , 0.3 mg;  $\text{Na}_2\text{WO}_4 \cdot 2\text{H}_2\text{O}$ , 0.4 mg; The final pH was adjusted to 7.

Medium A (for 1L): glycerol, 10 g; NH<sub>4</sub>Cl, 0.5 g; KCl, 0.3 g; NaH<sub>2</sub>PO<sub>4</sub>·2H<sub>2</sub>O, 3.2 g; Na<sub>2</sub>HPO<sub>4</sub>, 4.5 g; Na<sub>2</sub>SO<sub>4</sub>, 0.1 g; MgCl<sub>2</sub>·6H<sub>2</sub>O, 0.15 g; cysteine.HCl, 0.2 g; 10 mL trace metal solution. The final pH was adjusted to 6.5.

Medium B (for 1L): NH<sub>4</sub>Cl, 1.5 g; KCl, 0.1 g; NaH<sub>2</sub>PO<sub>4</sub>·2H<sub>2</sub>O, 0.7 g; NaAcO, 0.82 g; NaHCO<sub>3</sub>, 2.5 g; resazurine 1 mg; cysteine.HCl, 0.5 g; 10 mL of trace metal solution; Na<sub>2</sub>-fumarate, 8 g. The final pH of the medium was 6.8.

Medium C (for 1L): glycerol, 10 g; NH<sub>4</sub>Cl, 2 g; KCl, 0.75 g; NaH<sub>2</sub>PO<sub>4</sub>·2H<sub>2</sub>O, 3.2 g; Na<sub>2</sub>HPO<sub>4</sub>, 4.5 g; NaAcO, 0.82 g; Na<sub>2</sub>SO<sub>4</sub>, 0.28 g; MgCl<sub>2</sub>·6H<sub>2</sub>O, 0.26 g; cysteine.HCl, 0.2 g; 10 mL of trace metal solution. The final pH of the medium was 6.9.

All media were 99.995 % -N<sub>2</sub> sparged, pH adjusted, cysteine amended and autoclaved before adding 10 mL/L Wolfe's vitamin solution (Wolin et al. 1963), and fumarate if needed. 110-mL serum bottles (50 mL working volume) or 600-mL flasks (400 mL working volume) were used.

#### *Experimental coculture setup*

*G. sulfurreducens* PCA DSM12127 was purchased from DSMZ (Braunschweig, Germany) and was cultivated in medium B in 400 mL flasks. The pre-culture was centrifuged (4250 g 12 min) and washed with medium C. After the recentrifugation (4250 g 12 min), and the resuspension, it was inoculated all at once with the partner bacteria in medium C (final concentration ×2.7). A fraction of the resuspension was inoculated in medium B (50 mL) to check the viability of the cells. The concentration of *C. pasteurianum* at the beginning of the cocultures was around 5×10<sup>6</sup> cells/mL and the concentration of *G. sulfurreducens* was around 5×10<sup>9</sup> cells/mL.

*C. pasteurianum* DSM525 was purchased from DSMZ (Braunschweig, Germany) and was cultivated in DSM medium 54b and subcultured in medium A at least twice to remove residual yeast extract before inoculation 1/50 in medium C with or without *G. sulfurreducens*.

All bacteria were cultured in a shaking incubator at 35 °C (optimal temperature for *G. sulfurreducens* DSM12127). All manipulations were performed using Hungate-type techniques modified by Miller (see techniques in Miller and Wolin 1974).

The entire glycerol has always been consumed at the end of the fermentations. On-line pressure was monitored every 30 minutes by a micro-gas chromatography  $\mu$ GC-3000 (SRA Instruments, France).

#### *Analytical methods*

Metabolites were sampled at initial ( $t_0$ ) and final (after 48 to 96 h) stage of growth, and were quantified using a High Pressure Liquid Chromatography (Dionex Ultimate 3000). Aminex HPX-87H column (BioRad Cat No. 125-0140) with a pre-column Cation H (BioRad Cat No. 125-0129) were heated at 45 °C. Mobile phase was  $\text{H}_2\text{SO}_4$  4.1 mM at 0.3 mL/min, analysed through a refractometer (Waters 2414).

Gases were analysed at final stage with a Gas Chromatography (PerkinElmer Clarus 580) with a Rt-U-BOND column (RESTEK Cat No. 19752 30m x 0.32mm x 10 $\mu$ m) for  $\text{CO}_2$  and a Rt-Msieve 5Å column (RESTEK Cat No. 19722 30m x 0.32mm x 30 $\mu$ m) for  $\text{N}_2$ ,  $\text{O}_2$  and  $\text{H}_2$ . Mobile phase was argon (3.5 bars) and the detector was a thermal conductivity detector. Temperatures of the injector, oven and detector were 250, 60 and 150 °C respectively.

Absorbance spectra were recorded with a UV-visible UV-2501 PC spectrometer (Shimadzu, Nakagyō-ku, Japan) with plastic cuvettes.

Ammonium quantification was assessed using LCK302 tubes (Hach, Düsseldorf, Germany) and DR3900 spectrometer (Hach).

#### *Molecular biology techniques*

RNA was extracted using Qiagen RNeasy Mini kit (Qiagen Cat No./ID 74104). Cells (1.4 mL for *C. pasteurianum* or 1 mL for cocultures) were harvested at a given pressure of the flasks (1.2 bar, *i.e.* during the first hours of exponential growth) and put in 1.6 mL of RNA Protect Bacteria Reagent (Qiagen Cat No./ID 76506) 5 minutes before having been centrifuged 5000 g 10 min. The pellet was stored at -80 °C. 20  $\mu$ L of proteinase K (Qiagen Cat No./ID 19131) and 200  $\mu$ L Tris-EDTA-lysozyme buffer (30 mM Tris – 1 mM EDTA, pH 8, lysozyme 15 g/L) were added. The mix was incubated 10 min with 10 s vortex every 2 min before adding 1300  $\mu$ L RLT –  $\beta$ -mercaptoethanol (1 %) buffer and transferring into lysis matrix E (MPBio). FastPrep-24 5G (MPBio) was used to lyse the cells (40 s at 6 m/s). The

supernatant, after a 12,300 g 30 s centrifugation, was transferred into 1040  $\mu$ L absolute ethanol and the mix was loaded onto the kit column. A 350  $\mu$ L RW1 wash was followed by the adding of DNase (Qiagen Cat No./ID 79254) – RDD buffer (10-70  $\mu$ L). After a 12 min incubation, 350  $\mu$ L RW1 buffer was added (5 min incubation) and eluted, before a 500  $\mu$ L RPE buffer wash. RNAs were finally eluted in 50  $\mu$ L RNase-free water and stored at -80 °C. Nucleic acids were quantified with a microplate reader Spark (Tecan, Switzerland). Their concentrations were around 100 and 400 ng/ $\mu$ L for *C. pasteurianum* and coculture respectively.

DNA was extracted using Fast DNA Spin Kit for Soil (MPBio) and following the manufacturer's instructions starting with 2 mL samples. Lysis was performed with a FastPrep-24 5G (MPBio) 40 s at 6 m/s speed. Nucleic acids were quantified with a microplate reader Spark (Tecan). Quantitative PCR were conducted as in Moscoviz et al. (2017a) to count the number of cells, knowing that *C. pasteurianum* has 10 copies of 16S DNA.

#### *RNA sequencing*

RNAseq was performed at the GeT-PlaGe core facility, INRA Toulouse, as previously described (Péden et al. 2019), using one lane in one flow cell of a HiSeq3000 Illumina sequencer. Two quadruplicates were sequenced.

Raw data are available under the SRA accession PRJNA707372.

#### *RNA data analysis*

RNA sequencing data were analysed using the Genotoul calculation cluster. Reads were FastQC-checked (<https://www.bioinformatics.babraham.ac.uk/>) before a TrimGalore (<https://www.bioinformatics.babraham.ac.uk/>) trimming (stringency 3). The SortMeRNA package (Kopylova et al. 2012) was used to fuse the paired reads and to remove 5S, 16S and 23S RNA (according to GenBank sequences NZ\_CP009268.1 and NC\_002939.5). Around 90 % (*C. pasteurianum*) to 97 % (coculture) reads were removed at this stage. Alignment was then performed using bwa mem functions (Li and Durbin 2009; Li 2013) with Poehlein et al. annotation (NCBI assembly GCF\_000807255.1; Poehlein et al. 2015). SamTools (Li et al. 2009) and Integrative Genomics Viewer

(Robinson et al. 2011) were used for visualisation. Read counts were obtained with the FeatureCounts module (Liao et al. 2014; 50 % overlap for attribution, non paired-reads). Around 90 % of the reads were unambiguously assigned to *C. pasteurianum* genes (leading from 2.4 to 6.3 million reads per samples). The remaining reads were essentially constituted of reads overlapping 2 annotated genes (operon), reads in gene's 5'-untranslated regions or reads attributed to *G. sulfurreducens*.

Further analyses were done under R environment (<https://www.r-project.org/>, version 3.6). DESeq2 suite (<https://bioconductor.org/packages/release/bioc/html/DESeq2.html>; Love et al. 2014) was used to perform differential expression analysis (apeglm shrinkage of Zhu et al. 2019); pre-filtering: 10 reads per gene). A set of 3962 genes (out of 4085 annotated *C. pasteurianum* genes) were thus compared. Genes were considered differentially expressed if they were twice more or twice less expressed. Blast2GO software (Conesa et al. 2005; <https://www.blast2go.com/>) allowed to attribute Gene Ontology terms to proteins of *C. pasteurianum* with the following parameters: blastp-fast tool, 20 BLAST hits, against firmicutes, only proteins having at least a mean of 10 reads attributed. TopGO suite (Alexa et al. 2006) allowed then for Gene Ontology terms enrichment, using the classic algorithm with nodesize 5. Redundant terms are not shown in this article.

## Results

### **Effect of cell physiological state on *C. pasteurianum* – *G. sulfurreducens* interaction**

The first objective was to assess the culture conditions favourable to a successful *Geobacter sulfurreducens* – *Clostridium pasteurianum* interaction on glycerol. A successful interaction is characterized by a metabolic shift of *C. pasteurianum* from butanol to 1,3-propanediol, as reported by Moscoviz et al. (2017a). In the latter work, the physiological status of the two bacteria before performing the coculture was supposed to play a critical role in the establishment of the interaction.

The present experiment was performed by mixing simultaneously *C. pasteurianum* and *G. sulfurreducens* sampled from pre-cultures at different physiological states: exponential-, stationary- or late sporulating-phase cells, in medium containing only glycerol and acetate as carbon sources for *C.*

*pasteurianum* and *G. sulfurreducens* respectively. *G. sulfurreducens* was therefore deprived from electron acceptors and was thought to discharge its electrons to *C. pasteurianum*. The marker used to assess both the establishment and the strength of the bacterial interaction was the nature of the metabolic change. Indeed, *C. pasteurianum* produced more 1,3-propanediol (+37 %) and acetate, and less butanol (−16 %) and ethanol as a result of the interaction with *G. sulfurreducens* (Moscoviz et al. 2017a). All these metabolites were thus quantified at the end of the fermentation.

The fermentation profiles showed a variation in the concentrations of all tested metabolites, and this variation was in line with what would be expected from a successful interaction (Moscoviz et al. 2017a). The results confirmed that the physiological state of the bacteria at the beginning of the coculture was critical for the establishment and the strength of the interaction between them. Indeed, 2- to 5-day pre-culture of *G. sulfurreducens* (exponential and late-exponential growing phases) was optimal to favour the interaction (see Fig. 1a). In particular, a +76% increase in propanediol yield was observed in cocultures inoculated with 5-day *G. sulfurreducens* pre-cultures, whereas a +12 % only was seen with 9-day pre-cultures. In contrast, the metabolic change was more pronounced with aged *C. pasteurianum* pre-culture (see Fig. 1b). Indeed, a +160 % in propanediol yield was reached with cocultures inoculated with *C. pasteurianum* pre-cultures at late sporulating-phase (>1.5-day old), whereas a +29% only was observed with exponential-phase cells (grown overnight for 18 h).

In conclusion, the best condition was to use *C. pasteurianum* cells from a pre-culture in the late sporulating-phase and *G. sulfurreducens* cells from a pre-culture in exponential phase.

### ***C. pasteurianum* shows earlier and faster growth in coculture**

To evaluate the impact of the interaction on cellular growth, the number of cells of both bacterial species were measured by quantitative PCR and compared at final stage of growth (see Figure S1). *C. pasteurianum* growth was not affected in any coculture conditions and no significant growth of *G. sulfurreducens* was observed.

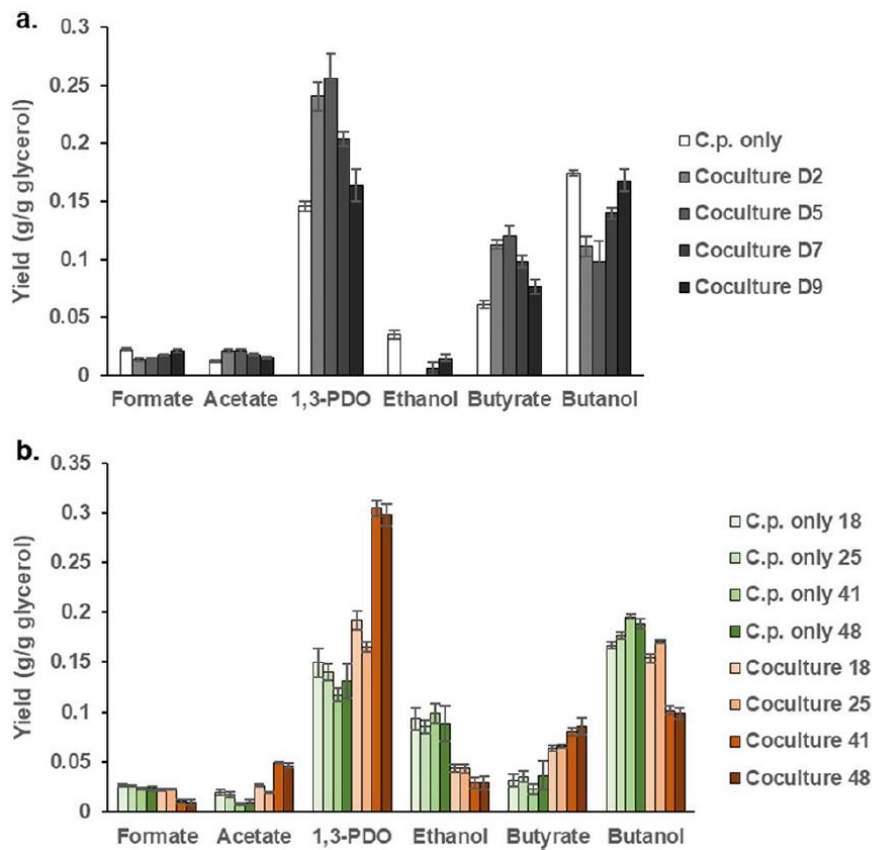


**Fig. 1** Fermentation profiles of *C. pasteurianum* alone vs. cocultured with *G. sulfurreducens*. a. The coculture was inoculated with *G. sulfurreducens* pre-cultures whose age ranged from 2 days (D2, exponential-phase cells) to 5 days (D5, late exponential-phase cells), 7 days (D7, stationary-phase cells) and 9 days (D9, late sporulating-phase cells). b. The coculture was inoculated with *C. pasteurianum* pre-cultures whose age ranged from 18 h (exponential-phase cells) to 25 h (stationary-phase cells), 41 h and 48 h (late sporulating-phase cells). Error bars are standard deviation of triplicates

In order to follow the kinetics of the fermentation process, the gas pressure of the reactors was measured all along the fermentation. Interestingly, the lag phase of the fermentation was shortened in cocultures when compared to *C. pasteurianum* grown alone (see Figure S2a). Old *C. pasteurianum* cells exhibited long lag phase up to 2-3 days when subcultured in fresh medium and this lag phase was substantially shortened down to 1 day when the same cells were instead inoculated along with *G. sulfurreducens*. Moreover, *C. pasteurianum* produced gas faster when in presence of *G. sulfurreducens* (rate of  $0.175 \pm 0.003 \text{ h}^{-1}$  in coculture vs.  $0.124 \pm 0.024 \text{ h}^{-1}$  with *C. pasteurianum* alone; standard deviation of

quadruplicates; see Figure S2b), which probably indicates a faster growth of *C. pasteurianum* in coculture.

### A mediated interaction between *C. pasteurianum* and *G. sulfurreducens*

Experiments were then conducted to know whether the interaction between the two species was mediated by a molecule or happens by cell-to-cell contact.

In the previous section, it was shown that *C. pasteurianum*'s metabolic profile changed when cultivated with *G. sulfurreducens*. Here we looked at the influence of *G. sulfurreducens* culture medium (spent medium) on *C. pasteurianum*. Indeed, in a different experiment, *G. sulfurreducens* was cultivated with acetate and fumarate as electron acceptor and, during the exponential phase, *C. pasteurianum* was added. In some of the bottles, *G. sulfurreducens* cells were removed (0.22  $\mu\text{m}$  filtration) before adding *C. pasteurianum*. Interestingly, a metabolic shift was observed with the spent medium of *G. sulfurreducens* and was similar to full cell cocultures, with for instance +114 % (coculture) and +92 % (spent medium culture) increases in 1,3-propanediol content (see Fig. 2).

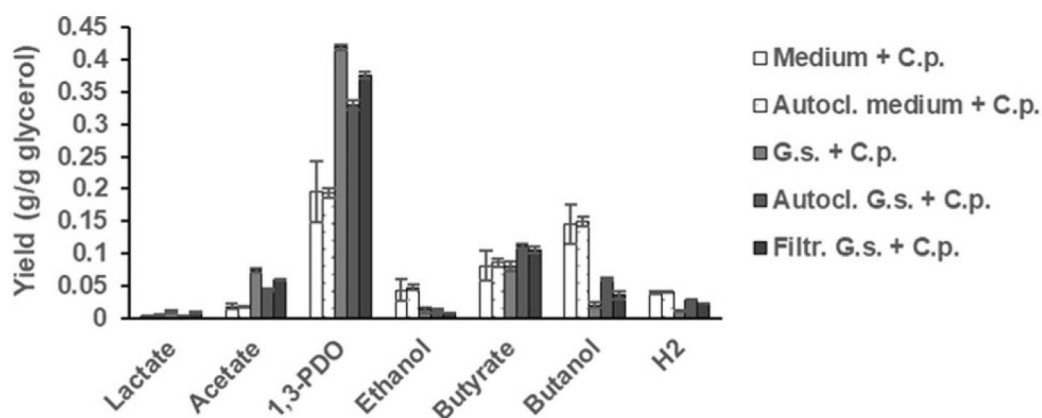


**Fig. 2** Metabolic profiles of *C. pasteurianum* at the end of the fermentation. Media were supplemented with fumarate and inoculated or not with *G. sulfurreducens*. After 2 days, some media were autoclaved or 0.22- $\mu\text{m}$  filtered. *C. pasteurianum* was then added. Error bars are standard deviation of quadruplicates.

The presence of *G. sulfurreducens* cells was therefore not necessary to induce changes in *C. pasteurianum* metabolic profile. This observation supports an interaction mechanism relying on a shuttle molecule.

*G. sulfurreducens* culture supernatants (0.22- $\mu$ m filtered) were analysed by UV-visible spectrometry to look for a shuttle molecule. An absorption peak at 408 nm was found, which moved to 398 nm when the samples were air-oxidized (see Fig. 3). This trait might be attributed to c-type cytochromes as previously proposed by Bansal et al. (2013) and Seeliger et al. (1998).

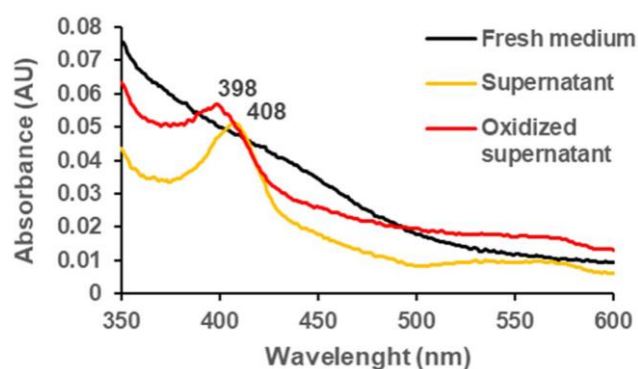


**Fig. 3** UV-visible spectrogram of *G. sulfurreducens* spent medium (0.22- $\mu$ m filtered, raw or air-oxidised) after 2 days of culture compared to fresh medium

*C. pasteurianum* is known to harbour different metabolic patterns when iron concentration drops, producing more propanediol and lactate, and less butanol (Dabrock et al. 1992; Groeger et al. 2017). A possible scheme could be a consumption of iron by *G. sulfurreducens*, that makes *C. pasteurianum* change its metabolism. However, no lactate was observed in any culture, whereas lactate accumulation is expected as an evidence for iron limitation (Dabrock et al. 1992; Utesch et al. 2019). Moreover, adding iron (in the form of  $\text{Fe}^{\text{II}}$ ) to the cultures did not prevent the metabolic shift (see Figure S3). Addition of other metals like the iron competitor cobalt (Dulay et al. 2020) or chelated cobalt (vitamin B<sub>12</sub> or cyanocobalamin) did not induce metabolic change of *C. pasteurianum* (see Figure S4).

Cysteine was proposed as electron acceptor for *G. sulfurreducens* (Kaden et al. 2002) and could be part of the interaction between the two species. However, *C. pasteurianum* metabolic change still occurred in fermentation medium with no cysteine supplementation (see Figure S5).

## **Translation, electron transfer, cobalamin synthesis and nitrogenase expression modification in *C. pasteurianum* when interacting with *G. sulfurreducens* highlighted by RNAseq analysis**

In order to better understand the mechanisms behind the metabolic change of *C. pasteurianum* in co-culture, RNA sequencing and differential expression analysis were performed on quadruplicate exponential-growth phase *C. pasteurianum* cells in presence or absence of *G. sulfurreducens* (metabolic profiles are available in Figure S6). Out of the 4085 *C. pasteurianum*'s annotated genes, 1028 were differentially expressed (*i.e.* twice more or twice less expressed) in coculture compared to pure culture. The details of the results are available in Table S1.

### *Global analysis of RNAseq data*

With the aim of assessing which functions of *C. pasteurianum* were modified in presence of *G. sulfurreducens*, it was first attempted to attribute functions to every genes of *C. pasteurianum*. All coding genes of *C. pasteurianum* were thus assigned to Gene Ontology (GO) terms (Ashburner et al. 2000; see Methods section). As a result, 2543 out of 3850 proteins were expected to have at least one molecular function, and 2117 at least one biological function. The remaining proteins were considered as of unknown function.

A Gene Ontology enrichment was then performed using TopGO functions suite (Alexa et al. 2006). It allowed assessing how strongly a specific molecular or biological function was modulated when *G. sulfurreducens* was present in the medium.

In terms of molecular functions (see Table 1), ribosome scaffolding appeared as the strongest modified function in presence of *G. sulfurreducens*, with 25 differentially expressed genes (out of 56 annotated in the genome; rank 1, Gene Ontology term #0003735, p-value of  $8.7 \times 10^{-5}$ ), 23 of which were upregulated (see the detailed proteins in Table S1). The same genes were also counted in the “structural molecule activity” term (see Table 1, rank 2). rRNA binding and tRNA binding enrichments support the hypothesis of a significant effect of *G. sulfurreducens* on *C. pasteurianum*'s translation machinery,

which seemed overexpressed. With a p-value of 0.017 and 9 differentially expressed genes, the electron transfer activity was also highly modified by the presence of *G. sulfurreducens*. Among these 9 genes, 8 were overexpressed (see Table S1).

In terms of biological functions (see Table 2), the most significantly modified process was the synthesis of cobalamin (ranks 1, 2, 3, 5 and 12), with half of the annotated metabolic pathway that was downregulated (see details on Table S1). Functions linked with multi-organism processes were also modified (see Table 2, ranks 6, 8, 13 and 18) notably through downregulated quorum sensing genes, and processes linked with translation (Table 2, ranks 4, 7, 10, 11, 14, 16 and 17) were overexpressed.

**Table 1** Top molecular functions of *C. pasteurianum* modified by *G. sulfurreducens* in coculture compared to *C. pasteurianum* grown alone (Gene Ontology enrichment)

Rank	GO ID	Term	Annotated	Significant <sup>a</sup>	Fisher <sup>b</sup>
1	GO:0003735	structural constituent of ribosome	56	25 (23/2)	$8.7 \times 10^{-5}$
2	GO:0005198	structural molecule activity	63	25 (23/2)	$8.0 \times 10^{-4}$
3	GO:0019843	rRNA binding	44	18 (16/2)	0.0029
4	GO:0000049	tRNA binding	22	10 (7/3)	0.011
5	GO:0009055	electron transfer activity	20	9 (8/1)	0.017
6	GO:0005506	iron ion binding	30	11 (7/4)	0.043
7	GO:0003796	lysozyme activity	7	4 (1/3)	0.044

<sup>a</sup> upregulated and downregulated genes are written in brackets (upregulated/downregulated).

<sup>b</sup> Fisher's exact test (p-value)

**Table 2** Top biological functions of *C. pasteurianum* modified by *G. sulfurreducens* in coculture compared to *C. pasteurianum* grown alone (Gene Ontology enrichment)

Rank	GO ID	Term	Annotated	Significant <sup>a</sup>	Fisher <sup>b</sup>
1	GO:0033013	tetrapyrrole metabolic process	29	15 (0/15)	2.6×10 <sup>-4</sup>
2	GO:0006766	vitamin metabolic process	51	21 (5/16)	8.8×10 <sup>-4</sup>
3	GO:0009235	cobalamin metabolic process	23	12 (0/12)	9.8×10 <sup>-4</sup>
4	GO:0043604	amide biosynthetic process	145	46 (38/8)	0.0015
5	GO:0051188	cofactor biosynthetic process	108	36 (14/22)	0.0019
6	GO:0051704	multi-organism process	21	10 (1/9)	0.0061
7	GO:0006412	translation	119	37 (30/7)	0.0062
8	GO:0002376	immune system process	5	4 (0/4)	0.0084
9	GO:0017144	drug metabolic process	111	34 (16/18)	0.011
10	GO:0032268	regulation of cellular protein metabolic process	8	5 (1/4)	0.013
11	GO:0044267	cellular protein metabolic process	244	65 (33/32)	0.019
12	GO:0006824	cobalt ion transport	6	4 (0/4)	0.021
13	GO:0098542	defense response to other organism	6	4 (0/4)	0.021
14	GO:1901566	organonitrogen compound biosynthetic process	385	96 (62/34)	0.030
15	GO:0000041	transition metal ion transport	16	7 (3/4)	0.036
16	GO:0019538	protein metabolic process	357	89 (35/54)	0.037
17	GO:1901564	organonitrogen compound metabolic process	682	159 (73/86)	0.061
18	GO:0044419	interspecies interaction between organisms	11	5 (1/4)	0.063
19	GO:0048518	positive regulation of biological process	11	5 (1/4)	0.063
20	GO:0006730	one-carbon metabolic process	8	4 (3/1)	0.068
21	GO:0055080	cation homeostasis	8	4 (3/1)	0.068
22	GO:0022900	electron transport chain	29	10 (9/1)	0.069

<sup>a</sup> upregulated and downregulated genes are written in brackets (upregulated/downregulated).

<sup>b</sup> Fisher's exact test (p-value)

### *Study of the most differentially expressed genes*

Aside from this global analysis, the most differentially expressed genes were studied (see Table 3). The top genes are part of a vanadium-nitrogenase cluster (nifH6, vnfDGKEN), which was upregulated up to 90 fold in presence of *G. sulfurreducens*. Some metal transporters were also upregulated (arsB, feoB, CLPA\_RS10690). The central metabolism was deeply modified, downregulating the major alcohol dehydrogenase adhE (CLPA\_RS14065) whereas glycolysis and acetate kinase genes were upregulated (CLPA\_RS18665, CLPA\_RS05440, CLPA\_RS10110, CLPA\_RS10115). This is consistent with the metabolic shift observed in the presence of *G. sulfurreducens* where less production of ethanol and

butanol, and higher production of acetate were observed. Surprisingly, the 1,3-propanediol synthesis operon (CLPA\_RS11050 to CLPA\_RS11085) was not differentially expressed whereas 1,3-propanediol was the most dysregulated metabolite. An extra-electron transporter, namely a b5-cytochrome of *C. pasteurianum* (CLPA\_RS02120) was 11-fold upregulated. As 40 % of the amino acids of *C. pasteurianum*'s b5-cytochrome are charged, the protein is probably located in the cytoplasm.

Only two differentially expressed proteins were predicted to be both involved in electron transport and membrane-bound: a downregulated ubiquinone oxidoreductase (CLPA\_RS16710) and a 5-fold overexpressed flavin mononucleotide (FMN)-binding polyferredoxin (CLPA\_RS05505). The latter protein possesses 8 extracellular flavin sites and 3 intracellular ferredoxin sites according to the InterPro tool (<https://www.ebi.ac.uk/interpro>; Blum et al. 2021), which is an indicator of a putative electron transfer between the extracellular space and the cytoplasm. This protein is clustered with a flavin adenine dinucleotide (FAD):protein FMN-transferase (CLPA\_RS05500, twice overexpressed) that is 40 % similar to the FmnB protein involved in electron transfer in *Listeria monocytogenes* (Light et al. 2018). This transferase probably flavinylate the FMN-binding polyferredoxin to allow for electron transfer, as pointed out in Light et al. (2018).

## Discussion

An interaction between *C. pasteurianum* and *G. sulfurreducens* leading to a metabolic shift of the fermentative species on glycerol was previously observed (Moscoviz et al. 2017a) and the mechanisms behind this interaction were here further investigated. The metabolic change induced by the interaction was reproduced, but neither an impact on the growth of *C. pasteurianum* nor a significant growth of *G. sulfurreducens* were here observed. In our study, *C. pasteurianum* seemed to grow faster and earlier in coculture, and the faster growth was confirmed by the translation upregulation in the RNA sequencing analysis. Therefore, the proposed parasitic interaction between these two species, as suggested by Moscoviz et al. (2017b) was not substantially supported by our observations.

**Table 3** The most differentially expressed ( $\log_2$ ) genes of *C. pasteurianum* in presence of *G. sulfurreducens*

Locus	Name	Diff. expr.	RPKM <sup>a</sup>	Function
CLPA_RS06895	vnfD	+6.49	198	Vanadium nitrogenase
CLPA_RS06890	nifH6	+6.14	150	Vanadium nitrogenase
CLPA_RS06905	vnfK	+5.44	85	Vanadium nitrogenase
CLPA_RS02330	arsB	+5.16	144	Metal transporter
CLPA_RS03505		-5.14	44	
CLPA_RS06910	vnfE	+4.79	45	Vanadium nitrogenase
CLPA_RS19295		-4.67	75	
CLPA_RS06900	vnfG	+4.63	68	Vanadium nitrogenase
CLPA_RS11440		-4.63	64	
CLPA_RS14065	adhE	-4.60	3099	Alcohol dehydrogenase
CLPA_RS13565		-4.47	163	
CLPA_RS06915	vnfN	+4.43	54	Vanadium nitrogenase
CLPA_RS02335		+4.43	195	Oxydoreductase (arsB operon)
CLPA_RS09700	agrA4	-4.42	21	Quorum sensing transcription regulator
CLPA_RS02895		-4.39	14	Cobalamin synthesis protein
CLPA_RS02560	feoB	+4.03	12	Iron II transporter
CLPA_RS06420		-3.99	1019	
CLPA_RS20100		-3.93	37	Membrane lysine
CLPA_RS18665		+3.88	1632	Glycerol dehydrogenase
CLPA_RS10690		+3.83	8	Metal transporter
CLPA_RS05440		+3.83	205	Glycerol-3-phosphate dehydrogenase
CLPA_RS16075		-3.78	14	
CLPA_RS18365		-3.68	18	
CLPA_RS00975		-3.65	34	
CLPA_RS01160		+3.64	196	Transposase endonuclease
CLPA_RS12215		+3.58	39	Fe-S protein
CLPA_RS13580		-3.55	415	
CLPA_RS02120		+3.51	63	Cytochrome b5
CLPA_RS09705	agrB	-3.50	11	Quorum sensing membrane transporter
CLPA_RS20995		-3.50	23	Citrate/malate metabolism regulation kinase

<sup>a</sup> Reads Per Kilobase and per Million, calculated before the DESeq2 normalisation

Interestingly, the modifications in metabolic profiles were dependent on the physiological status of both cells at the inoculation. It appeared that exponential-phase cells of *G. sulfurreducens* and late sporulating-phase cells of *C. pasteurianum* were the best conditions for the interaction to occur. This could be due to the low growth rate of *G. sulfurreducens*, unadapted to grow using non-canonical electron acceptors. This bacterium would then have extra time to produce a pool of interacting molecules while *C. pasteurianum* goes through its lag phase. Indeed, it appeared that the interaction between the two bacteria could be mediated by a molecule that was routinely produced by *G. sulfurreducens* when

grown on acetate and fumarate, as the presence of *G. sulfurreducens* cells were not mandatory for the metabolic change to be induced (see Fig. 2).

Traces of a molecule that could be attributed to a c-type cytochrome were seen in *G. sulfurreducens*'s spent medium making *C. pasteurianum* shift its fermentation profile. Consistently, production of soluble c-type cytochromes by *G. sulfurreducens* was elsewhere observed during growth phase (Seeliger et al. 1998), but their involvement in electron transfer was ruled out (Lloyd et al. 1999). Besides, the autoclaved medium, having thus non-functional linearized *G. sulfurreducens* proteins showed still a similar effect on *C. pasteurianum*, excluding the possibility of a protein-based interaction. Nonetheless, the interacting molecule could be a cobamide, as previously observed for *G. sulfurreducens* by Yan et al. (2012), or a heme derivative.

Therefore, whereas *G. sulfurreducens* probably used *C. pasteurianum* as electron acceptor, the metabolic change of the latter is probably mainly induced by a small molecule and not necessarily by the electron transfer itself.

Interestingly, RNA sequencing allowed identifying several genes and classes of genes from *C. pasteurianum* whose expressions were significantly impacted: the translation machinery, the electron transfer activity, the nitrogen fixation (all up-regulated), the cobalamin synthesis and bacterial interaction mechanisms (both downregulated).

Cobalamin is a corrinoid tetrapyrrole whose biosynthetic pathway diverts from heme synthesis (Fang et al. 2017). Cobalamin is used as a cofactor for 1,3-propanediol synthesis in *C. pasteurianum* (Macis et al. 1998), this metabolite being the main compound produced in coculture. Cobalamins are derived from cobamide, differing by the ligands flanking the cobalt (Sokolovskaya et al. 2020). Cobamides are known to be produced by *G. sulfurreducens* (Yan et al. 2012) and to be involved in several bacterial interaction (Sokolovskaya et al. 2020). Interestingly, the metabolic pathway of *Akkermansia muciniphila*, a gut bacterium, was reoriented in presence of a such compound, changing from succinate to propionate production (Belzer et al. 2017).

In our study, no metabolic change was observed when the cobamide molecule vitamin B<sub>12</sub> was added to *C. pasteurianum* cultures, but the ligands surrounding the cobamide are known to be specific for both

the supplier and the receiver (Yan et al. 2012; Sokolovskaya et al. 2020), and vitamin B<sub>12</sub> is probably not an efficient cobamide for *C. pasteurianum*.

Cobalt and cobamide were also proven to be essential for nitrogen fixation in *C. pasteurianum* (Nicholas et al. 1964). *C. pasteurianum* is a known nitrogen-fixing bacterium that has four nitrogenase complexes, one being an iron-only nitrogenase, one other a vanadium nitrogenase. Both are upregulated in our experiments (but the Fe-nitrogenase has a low expression, with RPKM = 10). Interestingly however, Fe- and V- nitrogenases are suspected to be unused when either ammonium is available or molybdenum is lacking, probably because they are less efficient than the usual molybdenum nitrogenase (Harwood 2020). Ammonium was neither limiting, nor lower in coculture batches than in pure culture ones ( $577 \pm 34$  mg/L NH<sub>4</sub><sup>+</sup> axenic vs.  $578 \pm 13$  mg/L in coculture, at the RNAseq sample time; N = 3). Thus, either *G. sulfurreducens* traps molybdenum, or another regulation system exists, which could be linked with cobamide, as previously suggested (Kliewer and Evans 1963; Evans and Kliewer 1964). Therefore, an upregulation of the V-nitrogenase complex was possibly a consequence of the cobamide dysregulation. Ammonium content at the end of the fermentation was not different when *G. sulfurreducens* was present ( $454 \pm 4$  mg/L NH<sub>4</sub><sup>+</sup> in coculture vs.  $451 \pm 4$  mg/L; N = 2). Therefore, the V-nitrogenase complex (~70-fold upregulated) probably did not fix high amounts of dinitrogen. It was reported that V-nitrogenase could be expressed on highly reduced substrates, dumping excess electrons in the form of H<sub>2</sub> (Luxem et al. 2020). However, less H<sub>2</sub> was produced in coculture batches (see Figure S6). The role of V-nitrogenase remains therefore unclear.

Considering all results a putative scheme of the interaction mechanisms was hypothesized as follows (see Fig. 4): *G. sulfurreducens* produces cobamides (or hemes) that possibly interfere with *C. pasteurianum*'s growth, in several possible ways. The excess of cobamide could downregulate the cobalamin metabolic pathway, as a tight retrocontrol, and upregulate the vanadium nitrogenase. The extra cobamide molecules from *G. sulfurreducens* could also boost *C. pasteurianum*'s 1,3-propanediol synthesis at the key cobamide-dependant enzyme glycerol dehydratase, while the 1,3-propanediol operon was not overexpressed. The cobamide's ligands are known to be important for this enzyme efficiency and auto-deactivation (Toraya 2000), and *G. sulfurreducens*' cobamide (Hazra et al. 2015) could induce less deactivation of the enzyme of *C. pasteurianum*. This could explain the higher

propanediol production observed. As a support of this hypothesis, no metabolic change was observed in fermentation medium supplemented with glucose instead of glycerol (see Figure S7), indicating that *G. sulfurreducens* interference occurs on an enzyme specific to the glycerol metabolism such as the glycerol dehydratase.

The electron transfer predicted in Moscoviz et al. (2017a) might not be linked with this putative cobamide-mediated interaction. Indeed, the cobalt atom trapped in the corrin is probably not involved in electron transfer, as its redox potentials are around  $-0.6$  V ( $\text{Co}^{\text{III}}/\text{Co}^{\text{II}}$ ) and  $+0.2$  V ( $\text{Co}^{\text{II}}/\text{Co}^{\text{I}}$ ) vs. standard hydrogen electrode (Dereven'kov et al. 2013). The electrical interaction (needed for *G. sulfurreducens* to produce cobamides or hemes) could instead occur via either direct or mediated electron transfer as previously observed for *G. sulfurreducens* (Lovley 2017; Huang et al. 2020). Based on the RNAseq data, it can be proposed that the electrons coming from *G. sulfurreducens* might be discharged in *C. pasteurianum* through a transmembrane FMN-binding polyferredoxin and cellular cytochrome b5 – rubredoxin interplay (Das and Ljungdahl 2003), all proteins being upregulated (5, 11 and 3 fold, respectively; see Fig. 4). These extra electrons could also participate to a lesser extent in the metabolic change observed, as seen when *C. pasteurianum* is cultivated on a cathode (Choi et al. 2014; Khosravanipour Mostafazadeh et al. 2016; Utesch et al. 2019). This would enhance the metabolic shift and explain the upregulation of acetate production and downregulation of ethanol and butanol syntheses. As first attempt of better understanding the mechanisms underlying the interaction between *C. pasteurianum* and electroactive bacteria, a putative interaction scheme was proposed in this study, even though this possible interaction mechanism needs confirmation through analysis of the cobamide molecule and use of mutant strains. This work opens new perspectives on interactions between fermentative and electroactive species in mixed culture fermentation setups to control end products formation.

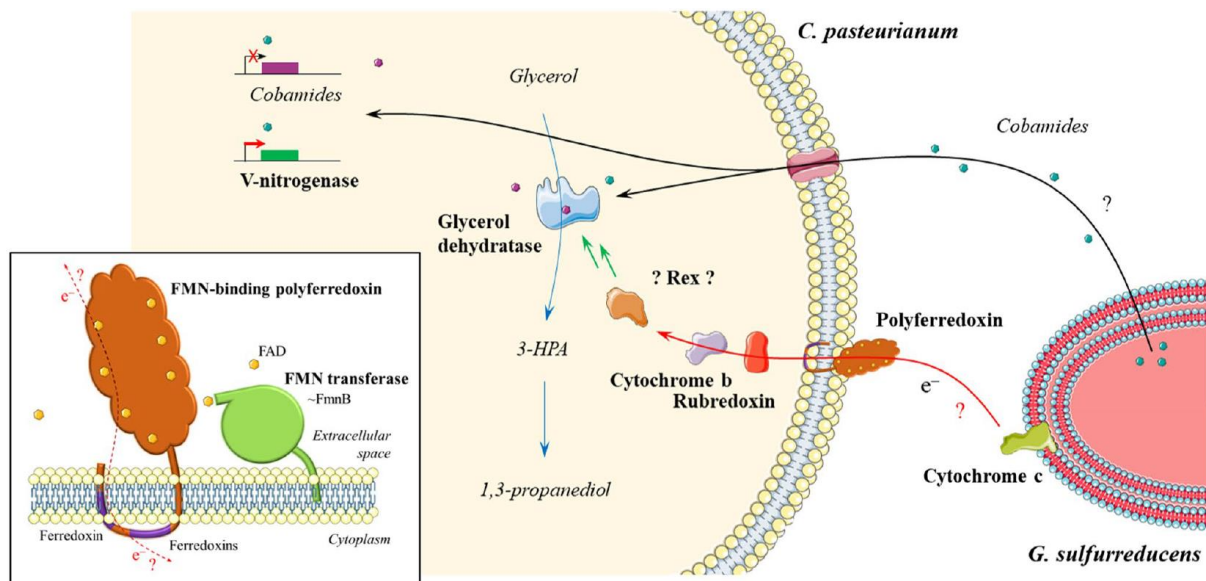


**Fig. 4** Recapitulative scheme of some of the putative interactions between *G. sulfurreducens* and *C. pasteurianum*. Cobamides produced by *G. sulfurreducens* could enter *C. pasteurianum* and compete for the cofactor site in the glycerol dehydratase, leading to more 1,3-propanediol synthesis. *G. sulfurreducens*' cobamides could downregulate *C. pasteurianum* cobamide synthesis and upregulate its vanadium nitrogenase. Electrons from *G. sulfurreducens* could be discharged to *C. pasteurianum* through its FMN-binding polyferredoxin and intracellular cytochrome b5 and rubredoxin that probably reduce a redox sensor, the latter inducing a general metabolic change. Inset: the FMN-binding polyferredoxin could be flavinylated by a FAD:protein FMN-transferase similar to the FmnB protein of Light et al. (2018) and thus transfer electrons between its extracellular flavins and intracellular ferredoxins. The polyferredoxin was chosen to start at the start codon ATG (1052 aminoacids). Rex: redox-sensing protein. 3-HPA: 3-hydroxypropionaldehyde. FAD: Flavin adenine dinucleotide. FMN: Flavin mononucleotide

## Declarations

## Funding

MFPB was funded by a Consejo Nacional de Ciencia y Tecnología (CONACyT) postdoctoral grant. This work was partly funded by Institut National de Recherche pour l'Agriculture, l'Alimentation et l'Environnement (INRAE) division Microbiologie Chaîne Alimentaire (MICA).

## Competing interests

The authors have no relevant financial or non-financial interests to disclose.

## Ethical approval

This article does not contain any studies with human participants or animals performed by any of the authors.

## Availability of data and material

The datasets generated during the current study (raw RNAseq reads in fastq format) are available in the NCBI SRA repository PRJNA707372: <https://www.ncbi.nlm.nih.gov/bioproject/PRJNA707372>

## Code availability

Codes were taken from both DESeq2 and TopGO packages available at <http://bioconductor.org>.

## Authors' contributions

RB and MFPB designed the study, carried out the experiments and drafted the manuscript. GSC performed part of the microbiological analysis. EDLQ, ET and NB designed and coordinated the study and helped to draft the manuscript. All authors reviewed the manuscript.

## References

- Alexa A, Rahnenfuhrer J, Lengauer T (2006) Improved scoring of functional groups from gene expression data by decorrelating GO graph structure. *Bioinformatics* 22:1600–1607 . <https://doi.org/10.1093/bioinformatics/btl140>
- Ashburner M, Ball CA, Blake JA, Botstein D, Butler H, Cherry JM, Davis AP, Dolinski K, Dwight SS, Eppig JT, Harris MA, Hill DP, Issel-Tarver L, Kasarskis A, Lewis S, Matese JC, Richardson JE, Ringwald M, Rubin GM, Sherlock G (2000) Gene Ontology: tool for the unification of biology. *Nat Genet* 25:25–29 . <https://doi.org/10.1038/75556>
- Bansal R, Helmus RA, Stanley BA, Zhu J, Liermann LJ, Brantley SL, Tien M (2013) Survival during long-term starvation: global proteomics analysis of *Geobacter sulfurreducens* under prolonged electron-acceptor limitation. *J Proteome Res* 12:4316–4326 . <https://doi.org/10.1021/pr400266m>
- Belzer C, Chia LW, Aalvink S, Chamlagain B, Piironen V, Knol J, de Vos WM (2017) Microbial metabolic networks at the mucus layer lead to diet-independent butyrate and vitamin B12 production by intestinal symbionts. *MBio* 8: . <https://doi.org/10.1128/mBio.00770-17>
- Blum M, Chang H-Y, Chuguransky S, Grego T, Kandasamy S, Mitchell A, Nuka G, Paysan-Lafosse T, Qureshi M, Raj S, Richardson L, Salazar GA, Williams L, Bork P, Bridge A, Gough J, Haft DH, Letunic I, Marchler-Bauer A, Mi H, Natale DA, Necci M, Orengo CA, Pandurangan AP, Rivoire C, Sigrist CJA, Sillitoe I, Thanki N, Thomas PD, Tosatto SCE, Wu CH, Bateman A, Finn RD (2021) The InterPro protein families and domains database: 20 years on. *Nucleic Acids Res* 49:D344–D354 . <https://doi.org/10.1093/nar/gkaa977>
- Choi O, Kim T, Woo HM, Um Y (2014) Electricity-driven metabolic shift through direct electron uptake by electroactive heterotroph *Clostridium pasteurianum*. *Sci Rep* 4:6961 . <https://doi.org/10.1038/srep06961>
- Conesa A, Gotz S, Garcia-Gomez JM, Terol J, Talon M, Robles M (2005) Blast2GO: a universal tool for annotation, visualization and analysis in functional genomics research. *Bioinformatics* 21:3674–3676 . <https://doi.org/10.1093/bioinformatics/bti610>
- Dabrock B, Bahl H, Gottschalk G (1992) Parameters affecting solvent production by *Clostridium pasteurianum*. *Appl Environ Microbiol* 58:1233–1239 . <https://doi.org/10.1128/AEM.58.4.1233-1239.1992>
- Dams RI, Guilherme AA, Vale MS, Nunes VF, Leitão RC, Santaella ST (2016) Fermentation of residual glycerol by *Clostridium acetobutylicum* ATCC 824 in pure and mixed cultures. *Environ Technol* 37:2984–2992 . <https://doi.org/10.1080/09593330.2016.1173114>
- Das A, Ljungdahl LG (2003) Electron-transport system in acetogens. In: *Biochemistry and Physiology of Anaerobic Bacteria*. Springer-Verlag, New York, pp 191–204
- Dereven'kov IA, Salnikov DS, Makarov S V., Boss GR, Koifman OI (2013) Kinetics and mechanism of oxidation of super-reduced cobalamin and cobinamide species by thiosulfate, sulfite and dithionite. *Dalt Trans* 42:15307 . <https://doi.org/10.1039/c3dt51714d>
- Dulay H, Tabares M, Kashefi K, Reguera G (2020) Cobalt resistance via detoxification and

- mineralization in the iron-reducing bacterium *Geobacter sulfurreducens*. *Front Microbiol* 11: .  
<https://doi.org/10.3389/fmicb.2020.600463>
- Evans HJ, Kliever M (1964) Vitamin B12 compounds in relation to the requirements of cobalt for higher plants and nitrogen-fixing organisms. *Ann N Y Acad Sci* 112:735–755 .  
<https://doi.org/10.1111/j.1749-6632.1964.tb45052.x>
- Fang H, Kang J, Zhang D (2017) Microbial production of vitamin B12: a review and future perspectives. *Microb Cell Fact* 16:15 . <https://doi.org/10.1186/s12934-017-0631-y>
- Faustino MM, Fonseca BM, Costa NL, Lousa D, Louro RO, Paquete CM (2021) Crossing the wall: characterization of the multiheme cytochromes involved in the extracellular electron transfer pathway of *Thermincola ferriacetica*. *Microorganisms* 9:293 .  
<https://doi.org/10.3390/microorganisms9020293>
- Groeger C, Wang W, Sabra W, Utesch T, Zeng A-P (2017) Metabolic and proteomic analyses of product selectivity and redox regulation in *Clostridium pasteurianum* grown on glycerol under varied iron availability. *Microb Cell Fact* 16:64 . <https://doi.org/10.1186/s12934-017-0678-9>
- Harwood CS (2020) Iron-only and vanadium nitrogenases: fail-safe enzymes or something more? *Annu Rev Microbiol* 74:247–266 . <https://doi.org/10.1146/annurev-micro-022620-014338>
- Hazra AB, Han AW, Mehta AP, Mok KC, Osadchiy V, Begley TP, Taga ME (2015) Anaerobic biosynthesis of the lower ligand of vitamin B12. *Proc Natl Acad Sci* 112:10792–10797 .  
<https://doi.org/10.1073/pnas.1509132112>
- Huang L, Liu X, Ye Y, Chen M, Zhou S (2020) Evidence for the coexistence of direct and riboflavin-mediated interspecies electron transfer in *Geobacter* co-culture. *Environ Microbiol* 22:243–254 .  
<https://doi.org/10.1111/1462-2920.14842>
- IEA (2021) Net Zero by 2050 A roadmap for the global energy sector. Paris
- Kaden J, S. Galushko A, Schink B (2002) Cysteine-mediated electron transfer in syntrophic acetate oxidation by cocultures of *Geobacter sulfurreducens* and *Wolinella succinogenes*. *Arch Microbiol* 178:53–58 . <https://doi.org/10.1007/s00203-002-0425-3>
- Khosravanipour Mostafazadeh A, Drogui P, Brar SK, Tyagi RD, Le Bihan Y, Buelna G, Rasolomanana S-D (2016) Enhancement of biobutanol production by electromicrobial glucose conversion in a dual chamber fermentation cell using *C. pasteurianum*. *Energy Convers Manag* 130:165–175 . <https://doi.org/10.1016/j.enconman.2016.10.050>
- Kliever M, Evans HJ (1963) Cobamide coenzyme contents of soybean nodules & nitrogen fixing bacteria in relation to physiological conditions. *Plant Physiol* 38:99–104 .  
<https://doi.org/10.1104/pp.38.1.99>
- Kopylova E, Noé L, Touzet H (2012) SortMeRNA: fast and accurate filtering of ribosomal RNAs in metatranscriptomic data. *Bioinformatics* 28:3211–3217 .  
<https://doi.org/10.1093/bioinformatics/bts611>
- Li H (2013) Aligning sequence reads, clone sequences and assembly contigs with BWA-MEM
- Li H, Durbin R (2009) Fast and accurate short read alignment with Burrows-Wheeler transform. *Bioinformatics* 25:1754–1760 . <https://doi.org/10.1093/bioinformatics/btp324>
- Li H, Handsaker B, Wysoker A, Fennell T, Ruan J, Homer N, Marth G, Abecasis G, Durbin R (2009) The Sequence Alignment/Map format and SAMtools. *Bioinformatics* 25:2078–2079 .  
<https://doi.org/10.1093/bioinformatics/btp352>
- Liao Y, Smyth GK, Shi W (2014) featureCounts: an efficient general purpose program for assigning sequence reads to genomic features. *Bioinformatics* 30:923–930 .  
<https://doi.org/10.1093/bioinformatics/btt656>
- Light SH, Su L, Rivera-Lugo R, Cornejo JA, Louie A, Iavarone AT, Ajo-Franklin CM, Portnoy DA (2018) A flavin-based extracellular electron transfer mechanism in diverse Gram-positive bacteria. *Nature* 562:140–144 . <https://doi.org/10.1038/s41586-018-0498-z>
- Lloyd JR, Blunt-Harris EL, Lovley DR (1999) The periplasmic 9.6-kilodalton c-type cytochrome of *Geobacter sulfurreducens* is not an electron shuttle to Fe(III). *J Bacteriol* 181:7647–7649 .  
<https://doi.org/10.1128/jb.181.24.7647-7649.1999>
- Love MI, Huber W, Anders S (2014) Moderated estimation of fold change and dispersion for RNA-seq data with DESeq2. *Genome Biol* 15:550 . <https://doi.org/10.1186/s13059-014-0550-8>
- Lovley DR (2017) Syntrophy goes electric: Direct interspecies electron transfer. *Annu Rev Microbiol* 71:643–664 . <https://doi.org/10.1146/annurev-micro-030117-020420>

- Luxem KE, Kraepiel AML, Zhang L, Waldbauer JR, Zhang X (2020) Carbon substrate re-orders relative growth of a bacterium using Mo-, V-, or Fe-nitrogenase for nitrogen fixation. *Environ Microbiol* 22:1397–1408 . <https://doi.org/10.1111/1462-2920.14955>
- Macis L, Daniel R, Gottschalk G (1998) Properties and sequence of the coenzyme B12-dependent glycerol dehydratase of *Clostridium pasteurianum*. *FEMS Microbiol Lett* 164:21–8 . <https://doi.org/10.1111/j.1574-6968.1998.tb13062.x>
- Miller TL, Wolin MJ (1974) A serum bottle modification of the Hungate technique for cultivating obligate anaerobes. *Appl Microbiol* 27:985–987 . <https://doi.org/10.1128/AM.27.5.985-987.1974>
- Monteiro MR, Kugelmeier CL, Pinheiro RS, Batalha MO, da Silva César A (2018) Glycerol from biodiesel production: Technological paths for sustainability. *Renew Sustain Energy Rev* 88:109–122 . <https://doi.org/10.1016/j.rser.2018.02.019>
- Moscoviz R, de Fouchécour F, Santa-Catalina G, Bernet N, Trably E (2017a) Cooperative growth of *Geobacter sulfurreducens* and *Clostridium pasteurianum* with subsequent metabolic shift in glycerol fermentation. *Sci Rep* 7:44334 . <https://doi.org/10.1038/srep44334>
- Moscoviz R, Flayac C, Desmond-Le Quémener E, Trably E, Bernet N (2017b) Revealing extracellular electron transfer mediated parasitism: energetic considerations. *Sci Rep* 7:7766 . <https://doi.org/10.1038/s41598-017-07593-y>
- Moscoviz R, Toledo-Alarcón J, Trably E, Bernet N (2016) Electro-fermentation: how to drive fermentation using electrochemical systems. *Trends Biotechnol* 34:856–865 . <https://doi.org/10.1016/j.tibtech.2016.04.009>
- Moscoviz R, Trably E, Bernet N (2018) Electro-fermentation triggering population selection in mixed-culture glycerol fermentation. *Microb Biotechnol* 11:74–83 . <https://doi.org/10.1111/1751-7915.12747>
- Nicholas DJD, Fisher DJ, Redmond WJ, Osborne M (1964) A cobalt requirement for nitrogen fixation, hydrogenase, nitrite and hydroxylamine reductases in *Clostridium pasteurianum*. *Nature* 201:793–795 . <https://doi.org/10.1038/201793a0>
- Okonkwo O, Escudie R, Bernet N, Mangayil R, Lakaniemi A-M, Trably E (2020) Bioaugmentation enhances dark fermentative hydrogen production in cultures exposed to short-term temperature fluctuations. *Appl Microbiol Biotechnol* 104:439–449 . <https://doi.org/10.1007/s00253-019-10203-8>
- Pankratova G, Leech D, Gorton L, Hederstedt L (2018) Extracellular electron transfer by the Gram-positive bacterium *Enterococcus faecalis*. *Biochemistry* 57:4597–4603 . <https://doi.org/10.1021/acs.biochem.8b00600>
- Paquete CM (2020) Electroactivity across the cell wall of Gram-positive bacteria. *Comput Struct Biotechnol J* 18:3796–3802 . <https://doi.org/10.1016/j.csbj.2020.11.021>
- Péden R, Poupin P, Sohm B, Flayac J, Giambérini L, Klopp C, Louis F, Pain-Devin S, Potet M, Serre R-F, Devin S (2019) Environmental transcriptomes of invasive dreissena, a model species in ecotoxicology and invasion biology. *Sci Data* 6:234 . <https://doi.org/10.1038/s41597-019-0252-x>
- Poehlein A, Grosse-Honebrink A, Zhang Y, Minton NP, Daniel R (2015) Complete genome sequence of the nitrogen-fixing and solvent-producing *Clostridium pasteurianum* DSM 525. *Genome Announc* 3:1997–1998 . <https://doi.org/10.1128/genomeA.01591-14>
- Robinson JT, Thorvaldsdóttir H, Winckler W, Guttman M, Lander ES, Getz G, Mesirov JP (2011) Integrative genomics viewer. *Nat Biotechnol* 29:24–26 . <https://doi.org/10.1038/nbt.1754>
- Rogelj J, Shindell D, Jiang K, Fifita S, Forster P, Ginzburg V, Handa C, Kheshgi H, Kobayashi S, Kriegler E, Mundaca L, Séférian R, Vilariño MV (2018) Mitigation pathways compatible with 1.5°C in the context of sustainable development. In: *Global Warming of 1.5°C. An IPCC Special Report on the impacts of global warming of 1.5°C above pre-industrial levels and related global greenhouse gas emission pathways, in the context of strengthening the global response to the threat of climate change.* p 82pp
- Seeliger S, Cord-Ruwisch R, Schink B (1998) A periplasmic and extracellular c-type cytochrome of *Geobacter sulfurreducens* acts as a ferric iron reductase and as an electron carrier to other acceptors or to partner bacteria. *J Bacteriol* 180:3686–3691 . <https://doi.org/10.1128/JB.180.14.3686-3691.1998>
- Sokolovskaya OM, Shelton AN, Taga ME (2020) Sharing vitamins: cobamides unveil microbial interactions. *Science (80- )* 369:1–9 . <https://doi.org/10.1126/science.aba0165>

- Toraya T (2000) Radical catalysis of B12 enzymes: structure, mechanism, inactivation, and reactivation of diol and glycerol dehydratases. *Cell Mol Life Sci* 57:106–127 .  
<https://doi.org/10.1007/s000180050502>
- Utesch T, Sabra W, Prescher C, Baur J, Arbter P, Zeng A (2019) Enhanced electron transfer of different mediators for strictly opposite shifting of metabolism in *Clostridium pasteurianum* grown on glycerol in a new electrochemical bioreactor. *Biotechnol Bioeng* 116:1627–1643 .  
<https://doi.org/10.1002/bit.26963>
- Wolin EA, Wolin MJ, Wolfe RS (1963) Formation of methane by bacterial extracts. *J Biol Chem* 238:2882
- Yan J, Ritalahti KM, Wagner DD, Löffler FE (2012) Unexpected specificity of interspecies cobamide transfer from *Geobacter* spp. to organohalide-respiring *Dehalococcoides mccartyi* strains. *Appl Environ Microbiol* 78:6630–6636 . <https://doi.org/10.1128/AEM.01535-12>
- Zhu A, Ibrahim JG, Love MI (2019) Heavy-tailed prior distributions for sequence count data: removing the noise and preserving large differences. *Bioinformatics* 35:2084–2092 .  
<https://doi.org/10.1093/bioinformatics/bty895>